Effect of TiO_2 Crystalline Phase Composition on the Physicochemical and Catalytic Properties of Pd/TiO_2 in Selective Acetylene Hydrogenation

Joongjai Panpranot,* Kunyaluck Kontapakdee, and Piyasan Praserthdam

Center of Excellence on Catalysis and Catalytic Reaction Engineering, Department of Chemical Engineering, Faculty of Engineering, Chulalongkorn University, Bangkok 10330, Thailand

Received: December 20, 2005; In Final Form: February 21, 2006

Pd/TiO_2 catalysts have been prepared using TiO_2 supports consisting of various rutile/anatase crystalline phase compositions. Increasing percentages of rutile phase in the TiO_2 resulted in a decrease in Brunauer−Emmett−Teller surface areas, fewer Ti^{3+} sites, and lower Pd dispersion. While acetylene conversions were found to be merely dependent on Pd dispersion, ethylene selectivity appeared to be strongly affected by the presence of Ti^{3+} in the TiO_2 samples. When TiO_2 samples with 0−44% rutile were used, high ethylene selectivities (58−93%) were obtained whereas ethylene losses occurred for those supported on TiO_2 with 85% or 100% rutile phase. X-ray photoelectron spectroscopy and electron spin resonance experiments revealed that a significant amount of Ti^{3+} existed in the TiO_2 samples composed of 0−44% rutile. The presence of Ti^{3+} in contact with Pd can probably lower the adsorption strength of ethylene resulting in an ethylene gain. Among the five catalysts used in this study, the results for Pd/TiO_2-R44 suggest an optimum anatase/rutile composition of the TiO_2 used to obtain high selectivity of ethylene in selective acetylene hydrogenation.

1. Introduction

Titanium dioxide (TiO_2) is a very useful material and has received great attention in catalysis research as a catalyst, a catalyst support, and a promoter. Due to the strong oxidizing power of its holes, high photostability, and redox selectivity, TiO_2 is one of the most popular and promising catalysts in photocatalytic applications.[1−3] In addition, as a catalyst support particularly in hydrogenation reactions, TiO_2 manifests a strong metal−support interaction (SMSI) with group VIII metals under high reduction temperatures (usually above 300 °C) resulting in an improved catalytic performance.[4,5] For example, Moon et al.[5] reported an improved selectivity for ethylene production in selective acetylene hydrogenation over TiO_2-modified Pd catalysts compared to Pd/SiO_2.

Naturally, TiO_2 has three main crystal structures: anatase, which tends to be more stable at low temperature; brookite, which is usually found in minerals and has an orthorhombic crystal structure, and rutile, which is the stable form at higher temperature.[6] Both rutile and anatase TiO_2 are tetragonal structures with unit cells consisting of 6 and 12 atoms, respectively.[7] Generally, anatase phase TiO_2 shows higher photocatalytic activity than other types of titanium dioxide due to its appropriate band gap energy that corresponds to UV light.[8] Since each crystal structure of TiO_2 possesses different physical properties, the use of TiO_2 with various polymorphs as catalyst supports might exhibit different characteristics and catalytic properties. Nevertheless only a few publications reported the effect of titania polymorph on such differences. Chary et al.[9] reported that MoO_3 dispersed better on anatase TiO_2 than when it was supported on rutile TiO_2. The number of surface Mo sites were directly correlated with the catalytic properties of the catalysts for ammoxidation of 3-picoline to nicotinonitrile. A recent study reveals that the SMSI of Pd/TiO_2 catalysts was also influenced by the titania polymorph.[10] Anatase TiO_2-supported palladium catalyst exhibited SMSI at lower temperatures than a rutile TiO_2-supported one. Jongsomjit et al.[11] have studied cobalt dispersion on TiO_2 and found that the presence of 19% rutile phase in titania facilitates the reduction of highly dispersed cobalt oxide to cobalt metal.

In this study, the physicochemical properties of TiO_2 and Pd dispersed on TiO_2 consisting of various rutile/anatase phase compositions were investigated by means of X-ray diffraction (XRD), N_2 physisorption, scanning electron microscopy (SEM), electron spin resonance (ESR), X-ray photoelectron spectroscopy (XPS), and pulse CO chemisorption methods. Furthermore, the catalytic properties of the Pd/TiO_2 catalysts were evaluated in the gas-phase selective hydrogenation of acetylene in excess ethylene.

2. Experimental Section

2.1. Preparation of TiO_2 and Pd/TiO_2 Catalyst Samples. TiO_2 supports with various rutile/anatase phase compositions were obtained by calcinations of pure anatase titania (Aldrich) in air at temperatures between 900 and 1100 °C for 4 h. The high space velocity of air flow (16 000 h^{-1}) ensured the gradual phase transformation to avoid rapid sintering of the samples. Approximately 1% Pd/TiO_2 was prepared by the incipient wetness impregnation technique using an aqueous solution of the desired amount of $Pd(NO_3)_2$ (Wako). The catalysts were dried overnight at 110 °C and then calcined in N_2 flow 60 cm^3/min with a heating rate of 10 °C/min until the temperature reached 500 °C and then in air flow 100 cm^3/min at 500 °C for 2 h.

2.2. Catalyst Characterization. The Brunauer−Emmett−Teller (BET) surface areas of the samples were determined by N_2 physisorption using a Micromeritics ASAP 2000 automated system. Each sample was degassed under vacuum at <10 μm Hg in the Micromeritics ASAP 2000 at 150 °C for 4 h prior to

* Author to whom correspondence should be addressed. E-mail: joongjai.p@eng.chula.ac.th.

10.1021/jp057395z CCC: $30.25
Published on Web 03/25/2006

N_2 physisorption. The XRD spectra of the catalyst samples were measured from 20° to 80° 2θ using a Siemens D5000 X-ray diffractometer and Cu Kα radiation with a Ni filter. Electron spin resonance spectra were taken at −150 °C using a JEOL JES-RE2X spectrometer. Relative percentages of palladium dispersion were determined by pulsing carbon monoxide over the reduced catalyst. Approximately 0.2 g of catalyst was placed in a quartz tube in a temperature-controlled oven. The amounts of CO chemisorbed on the catalysts were measured using a Micromeritic Chemisorb 2750 automated system attached with ChemiSoft TPx software at room temperature. Prior to chemisorption, the sample was reduced in a H_2 flow at 500 °C for 2 h, then cooled to ambient temperature in a He flow. The particle morphology was obtained using a JEOL JSM-35CF scanning electron microscope operated at 20 kV. The XPS analysis was performed using an AMICUS photoelectron spectrometer equipped with a Mg Kα X-ray as a primary excitation and KRATOS VISION2 software. XPS elemental spectra were acquired with a 0.1 eV energy step at a pass energy of 75 kV. The C 1s line was taken as an internal standard at 285.0 eV. A temperature-programmed desorption (TPD) study was performed in a Micromeritic ChemiSorb 2750 automated system attached with ChemiSoft TPx software. Approximately 0.05 g of a calcined catalyst was placed in a quartz tube in a temperature-controlled oven and connected to a thermal conductivity detector (TCD). The catalyst was first reduced in H_2 flow at 100 cm^3/min for 1 h at 500 °C (using a ramp rate of 10 °C/min) and then cooled to room temperature. The catalyst surface was saturated with ethylene or CO by applying a high purity grade ethylene or CO at 60 mL/min for 3 h. Then the samples were flushed with helium while cooling to room temperature for about 1 h. The temperature-programmed desorption was performed with a constant heating rate of ca. 10 °C/min from 35 to 500 °C. The amount of desorbed ethylene or CO was measured by analyzing the effluent gas with a thermal conductivity detector.

2.3. Reaction Study. Selective acetylene hydrogenation was performed in a quartz tube reactor (i.d. 9 mm). Prior to the start of each run, the catalyst was reduced in H_2 at 500 °C for 2 h. Then the reactor was purged with argon and cooled to the reaction temperature, 40 °C. Feed gas composed of 1.46% C_2H_2, 1.71% H_2, 15.47% C_2H_6, and balanced C_2H_4 (Rayong Olefin Co., Ltd) and a GHSV of 5400 h^{-1} were used. The composition of product and feed stream were analyzed by a Shimadzu GC 8A equipped with a TCD and flame ionization detector (FID) (molecular sieve 5 Å and carbosieve S2 columns, respectively). Acetylene conversion as used herein is defined as moles of acetylene converted with respect to acetylene in feed. Ethylene selectivity is defined as the percentage of acetylene hydrogenated to ethylene over totally hydrogenated acetylene. The ethylene being hydrogenated to ethane (ethylene loss) is the difference between all the hydrogen consumed and all the acetylene that has been totally hydrogenated.

3. Results and Discussion

3.1. Properties of TiO_2 Consisting of Various Rutile/Anatase Phase Compositions. In this study, pure anatase titania was gradually transformed into rutile titania by calcination in air under temperatures ranging between 900 and 1010 °C for 4 h. XRD patterns of the calcined TiO_2 samples are shown in Figure 1. For the pure anatase titania, XRD peaks at 25°, 37°, 48°, 55°, 56°, 62°, 71°, and 75° 2θ were evident. XRD peaks for rutile phase at 28° (major), 36°, 42°, and 57° appeared after calcinations. The amount of rutile phase formed during calcinations depended on the temperature used and was calculated using

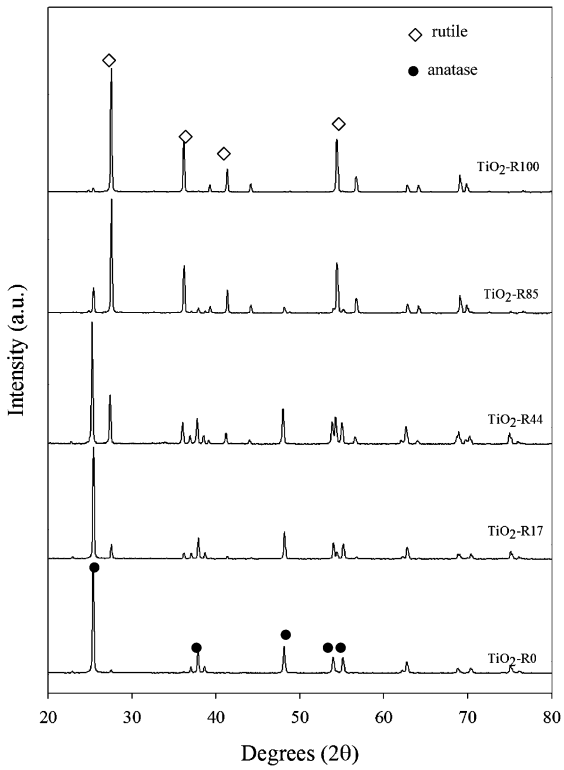

Figure 1. XRD patterns of TiO_2 samples.

the areas of the major anatase and rutile XRD peaks according to the method described by Jung et al.[12] as follows

$$\% \text{ rutile} = \frac{1}{\left[\left(\frac{A}{R}\right)0.884 + 1\right]} \times 100$$

where A and R are the peak areas for the major anatase (2θ = 25°) and rutile phase (2θ = 28°), respectively.

The titania samples consisting of 0, 17, 44, 85, and 100% rutile phase were named as TiO_2-R0, R17, R44m R85, and R100, respectively. Scanning electron micrographs of various titania samples are shown in Figure 2; agglomeration of the particles is clearly seen with increasing percentage of rutile phase in the TiO_2 samples. After being subjected to the thermal treatment (calcination), BET surface areas of the TiO_2 samples (Table 1) decreased essentially from 64.4 for R0 (pure anatase) to 18.3 m^2/g for R100 (pure rutile). The ESR spectra of the TiO_2 samples are shown in Figure 3. The signals of g values less than 2 were assigned to Ti^{3+} ($3d^1$).[13,14] No Ti^{3+} ESR signal was observed for TiO_2 consisting of ≥85% rutile phase. It is suggested that Ti^{4+} in the TiO_2 with higher percentages of rutile is more difficult to be reduced to Ti^{3+}. As rutile titania is more thermodynamically and structurally stable than anatase titania, the Ti^{3+} ions fixed in the surface lattice of anatase TiO_2 are easier to diffuse to the surface those in the surface lattice of rutile TiO_2.[10] The results in this study suggest a threshold limit of maximum percentage of rutile in the TiO_2 sample so that the presence of Ti^{3+} can be detected by the ESR technique.

The survey XPS spectra for pure rutile and anatase TiO_2 samples were recorded with a photon energy of 1256 eV (Mg Kα), the kinetic energies of the emitted electrons being in the range of 0−1000 eV. The core level XPS spectra of Ti 2p recorded from various TiO_2 samples (results not shown) show sharp and intense peaks at binding energies 464.2 and 458.5 eV, indicating of only Ti^{4+} in the TiO_2.[15,16] No Ti^{3+} XPS spectra

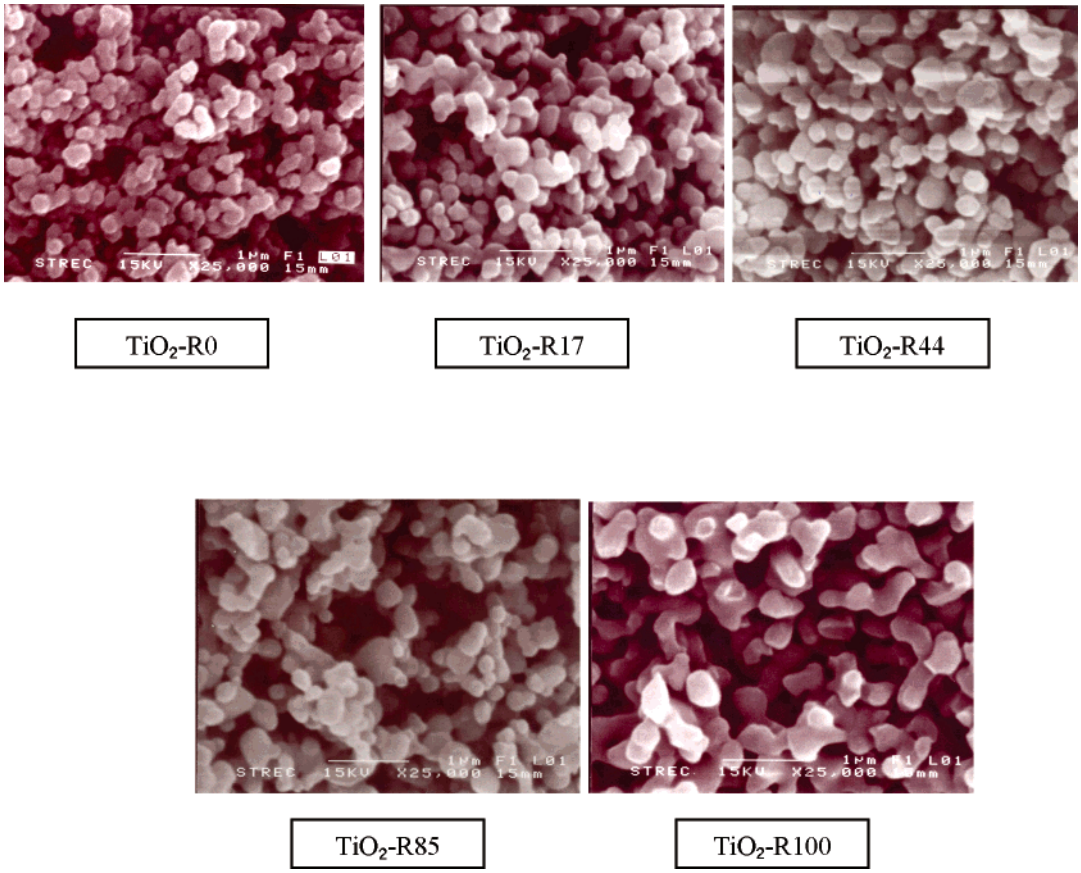

Figure 2. SEM micrographs of various TiO_2 samples.

TABLE 1: TiO_2 Samples Consisting of Various % Rutile

sample	% rutile	BET surface area (m^2/g)
TiO_2-R0	0	64.4
TiO_2-R17	17	38.6
TiO_2-R44	44	25.0
TiO_2-R85	85	23.5
TiO_2-R100	100	18.3

were seen for all the TiO_2 samples under these conditions. It is likely that there was an oxygen-rich layer near the surface of the TiO_2 particles, which is formed by oxygen adsorption and easy oxidation of the titanium surface.[17] To observe the reduced Ti species (i.e., Ti^{3+}, Ti^{2+}) that might exist in the bulk of the TiO_2 samples, TiO_2 surfaces were subjected to an argon-ion bombardment for 2 min. Ti 2p XPS spectra of the Ar^+-etched TiO_2 samples are illustrated in Figure 4. The presence of new Ti $2p^{1/2}$ and $2p^{3/2}$ peaks at lower binding energies of 461.2 and 456.5 eV indicated Ti^{3+} species in the TiO_2.[15,16,18,19] It was found that the intensities of Ti^{3+} for both Ti $2p^{1/2}$ and $2p^{3/2}$ peaks increased with decreasing percentages of the rutile phase. The results were found to be in accordance with our ESR results. Moreover, Ti 2p peaks indicative of Ti^{2+} species[17,19] were also observed at binding energies of 451.8 and 454.3 eV for TiO_2 samples with low percentages of the rutile phase.

3.2. Dispersion of Pd on the TiO_2 Surface. Dispersion of the active surface Pd on TiO_2 consisting of various rutile/anatase phase compositions was investigated by means of CO pulse chemisorption and XPS techniques, and the results are given in Table 2. Since palladium hydride can be formed in the presence of hydrogen, CO chemisorption is typically preferred rather than H_2 chemisorption for the measurement of active palladium surface with the assumption that one carbon monoxide

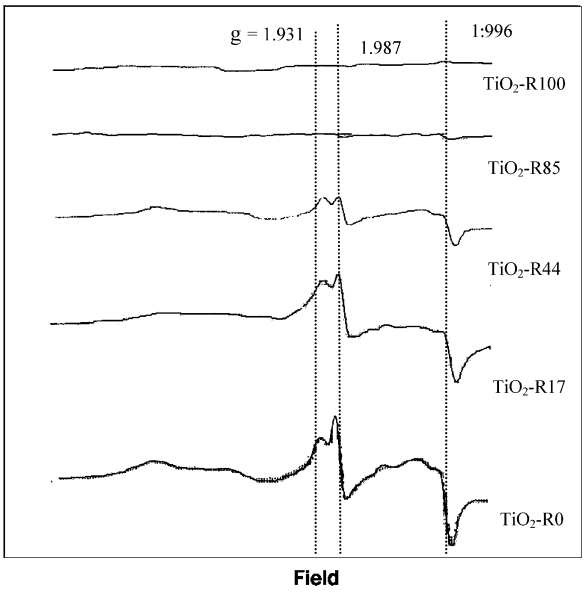

Figure 3. ESR spectra of TiO_2 samples.

molecule adsorbs on the palladium site.[20−25] The BET surface areas of the TiO_2-supported Pd catalysts were slightly less than that of the original TiO_2 supports suggesting that palladium was deposited in some of the pores of TiO_2. It would appear that the particle size and shape of the catalyst particles were not affected by impregnation of palladium (no changes in the particle size/shape). Since no XRD peaks of PdO or Pd^0 were observed for the catalyst samples after calcinations at 450 °C for 3 h, it suggests that palladium was highly dispersed on the titania surface (results not shown). It was found that as the percentage of the rutile phase increased from 0 to 100% the amount of CO

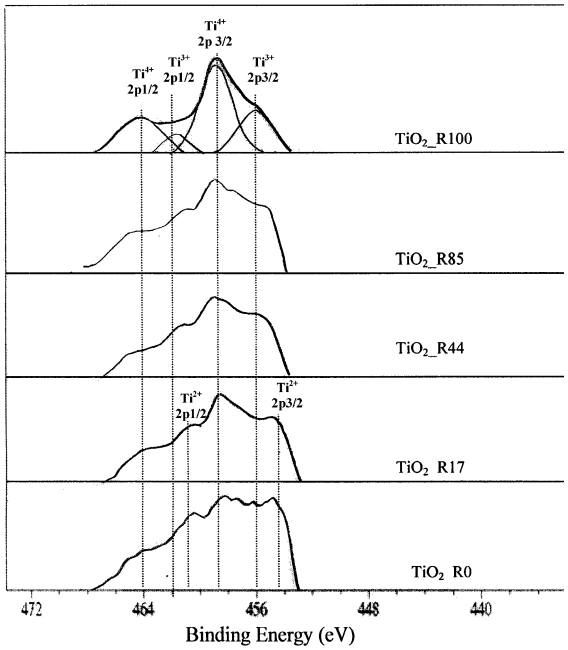

Figure 4. XPS Ti 2p spectra of TiO_2 samples after 2 min of etching by Ar^+.

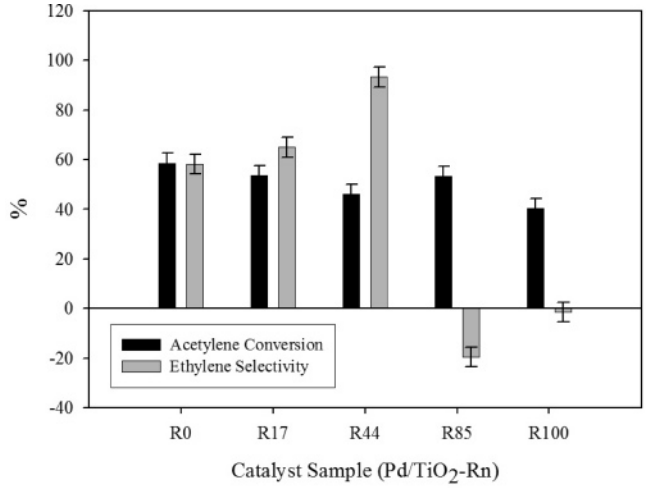

Figure 5. Catalytic performances of various Pd/TiO_2 catalysts in selective acetylene hydrogenation.

chemisorption decreased from 2.23×10^{18} to 1.55×10^{18} molecules of CO while the calculated average particle size of Pd^0 metal increased from 28.5 to 41.0 nm. Thus, the presence of rutile phase significantly decreased dispersion of palladium on the titania supports. XPS analysis revealed an increasing Pd surface concentration with increasing percentages of rutile up to ca. 44% rutile. Further increases in the percentage of the rutile phase did not result in a higher concentration of Pd on the TiO_2 surface and could lower the Pd surface concentration for pure rutile TiO_2.

3.3. Selective Acetylene Hydrogenation on Pd/TiO_2 Catalysts. To investigate the catalytic performance of Pd/TiO_2 catalysts consisting of various rutile phase percentages, selective hydrogenation of acetylene to ethylene was performed in a fixed bed flow reactor. Removal of a trace amount of acetylene in an ethylene feed stream is vital for the commercial production of polyethylene since acetylene acts as a poison to the polymerization catalysts. Figure 5 shows acetylene conversions and ethylene selectivities obtained from various Pd/TiO_2 catalysts. Acetylene conversions were in the range of 40−59% and were found to be merely dependent on the Pd dispersion. However, a rapid change of catalytic properties in terms of ethylene selectivity was observed. When the TiO_2 supports with rutile contents of 44% or less were employed, ethylene selectivities were positive varied from 58 to 93% with a maximum for the Pd/TiO_2-R44. On the contrary, ethylene selectivities became negative when Pd catalysts supported on TiO_2 consisting ≥85% rutile phase were used resulting in ethylene losses. Overhydrogenation of ethylene to ethane was likely to occur for such cases. Ethylene hydrogenation is usually believed to take place on the support by means of a hydrogen transfer mechanism.[26] There may be some relationship between the presence of Ti^{3+} ions in the TiO_2 supports and the high ethylene selectivity since only the Pd catalysts supported on TiO_2 with a significant amount of Ti^{3+} yielded high ethylene gains. This could probably be explained in terms of the SMSI effect. Generally, SMSI occurs for Pd/TiO_2 catalysts after reduction at high temperature, lowering the adsorption strength of ethylene on the catalyst surface; thus high ethylene selectivity can be obtained.[5] In this work, the amounts of CO adsorbed on the catalysts reduced at 500 °C were much smaller than those reduced at room temperature. Since the CO adsorption ability of the catalysts can be recovered (restored) so that the decline in the amount of CO adsorbed at high-temperature reduction was caused by an SMSI effect and not by metal sintering. Detailed experimental observation of the reversibility of the SMSI effect for group VIII metals in oxidizing atmospheres can be found in ref 27. It is also known that suppression of H_2 chemisorption occurs on such catalysts similar to that of CO. Recently, Fan et al. suggested that diffusion of Ti^{3+} from the lattice of anatase TiO_2 to surface Pd particles can lower the temperature to induce SMSI.[10]

The characteristics of the surface active sites of the catalysts were studied by means of the temperature-programmed desorption of CO and ethylene from 50 to 500 °C. The results are shown in Figures 6A and 6B, respectively. Similar profiles were found for both CO and ethylene temperature-programmed desorption in which two main desorption peaks were observed. Such results suggest that there were two different active sites on the catalysts, probably Pd and Ti^{3+} sites. Since the high-temperature peaks were diminished with increasing percentages of rutile in the TiO_2 supports, these peaks could be attributed to the adsorption on Ti^{3+} sites. The low-temperature peaks, therefore, were attributed to adsorption on Pd sites. Adsorption of CO on Ti^{3+} sites has also been observed by an IR study by Benvenutti et al.[28]

TABLE 2: Physicochemical Properties of Pd/TiO_2 Catalysts

sample	BET surface area (m^2/g)	CO chemisorption $\times 10^{18}$ (molecule CO/g catalyst)	Pd dispersion (%)	d_P Pd^0 (nm)	atomic concentration Pd/Ti
Pd/TiO_2-R0	44.5	2.23	3.93	28.5	0.084
Pd/TiO_2-R17	27.1	2.20	3.87	28.9	0.116
Pd/TiO_2-R44	20.1	1.66	2.92	38.3	0.196
Pd/TiO_2-R85	19.8	1.77	3.12	35.9	0.199
Pd/TiO_2-R100	17.2	1.55	2.73	41.0	0.168

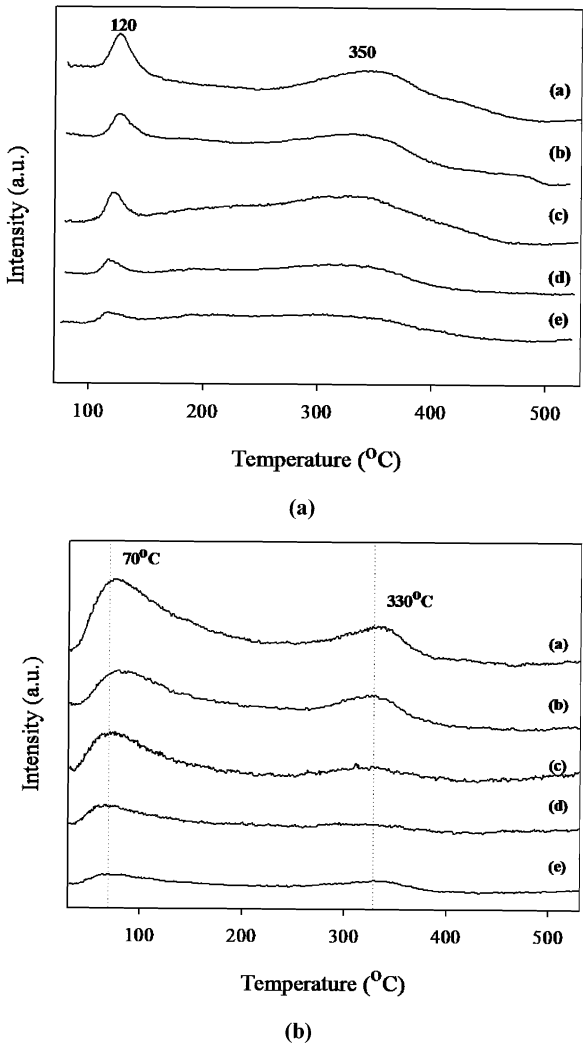

Figure 6. Temperature-programmed desorption of (A) CO and (B) C_2H_4 for the various Pd/TiO_2 catalysts: (a) Pd/TiO_2-R0, (b) Pd/TiO_2-R17, (c) Pd/TiO_2-R44, (d) Pd/TiO_2-R85, (e) Pd/TiO_2-R100.

In our study, we propose that ethylene can adsorb on Ti^{3+} sites and hydrogenate to ethane. However, simultaneously Ti^{3+} species that were in contact with the palladium surface promoted the SMSI effect and ethylene desorption.[10] Thus, without Ti^{3+} on the TiO_2 surface, low selectivity for ethylene was observed (as seen for the cases of Pd/TiO_2-R85 and Pd/TiO_2-R100) while with too many Ti^{3+} (that were not in contact with Pd) ethylene hydrogenation also occurred. Therefore, among the three catalysts with significant amounts of Ti^{3+} used in this study, Pd/TiO_2-R44 exhibited higher ethylene gains than Pd/TiO_2-R17 and Pd/TiO_2-R0, respectively. The proposed mechanism for acetylene hydrogenation on different types of active sites on Pd/TiO_2 catalysts is illustrated in a conceptual model in Figure 7. In a previous study from our group, two types of solvothermal-derived pure anatase TiO_2-supported Pd catalysts were prepared and studied in acetylene hydrogenation. It was found that the one containing a higher amount of Ti^{3+} exhibited slightly lower ethylene selectivity.[29] The results from the present study, however, emphasize the influence of Ti^{3+} present in the TiO_2 samples on their catalytic behavior; the results for Pd/TiO_2-R44 suggest the best (optimum) anatase/rutile composition of the TiO_2 used to obtain high selectivity of ethylene in selective acetylene hydrogenation.

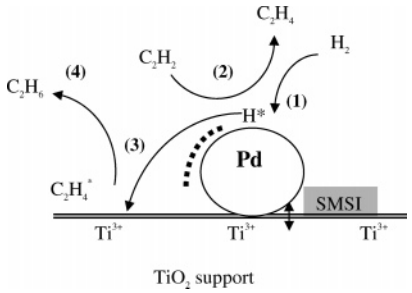

Figure 7. Conceptual model for selective acetylene hydrogenation mechanism on Pd/TiO_2 catalysts: (1) H_2 transfer from the metal to the support, (2) acetylene hydrogenation to ethylene followed by ethylene desorption, (3) adsorption of ethylene on Ti^{3+} sites, (4) hydrogenation of ethylene to ethane

4. Conclusions

The physicochemical and catalytic properties of Pd/TiO_2 catalysts can be significantly influenced by the anatase/rutile crystalline phase composition of the TiO_2 supports. Higher percentages of rutile in TiO_2 resulted in a decrease in BET surface areas and fewer Ti^{3+} sites. The presence of Ti^{3+} in the Pd/TiO_2 catalysts appeared to promote ethylene selectivity in selective acetylene hydrogenation when Ti^{3+} sites were in contact with Pd. Among the five crystalline phase compositions of titania used in this study, the one containing 44% rutile was found to be the best (optimum) composition to prepare TiO_2-supported Pd catalysts with high ethylene selectivity.

Acknowledgment. Financial support from the Thailand Research Fund, Rayong Olefins Co., Ltd., and the Graduate School of Chulalongkorn University is gratefully acknowledged.

References and Notes

(1) Ohtani, B.; Ogawa, Y.; Nishimoto, S. *J. Phys. Chem. B* **1997**, *101*, 3746.
(2) Stafford, U.; Gray, K. A.; Kamat, P. V. *J. Catal.* **1997**, *167*, 25.
(3) Herrmann, J.-M. *Catal. Today* **1999**, *53*, 115.
(4) Tauster, S. J.; Fung, S. C.; Garten, R. L. *J. Am. Chem. Soc.* **1978**, *100*, 170.
(5) Kang, J. H.; Shin, E. W.; Kim, W. J.; Park, J. D.; Moon S. H. *J. Catal.* **2002**, *208*, 310.
(6) Rao, C. N. R.; Yuganarasimhan, S. R.; Faeth, P. A. *Trans. Faraday Soc.* **1961**, *57*, 504.
(7) Stashans, A.; Lunell, S.; Grimes, R. W. *J. Phys. Chem. Solids* **1996**, *57*, 1293.
(8) Yin, H.; Wada, Y.; Kitamura, T.; Kambe, S.; Murasawa, S.; Mori, H.; Sakata, T.; Yanagida S. *J. Mater. Chem.* **2001**, *11*, 2694.
(9) Chart, K. V. R.; Bhaskar, T.; Seela, K. K.; Lakshmi, K. S.; Reddy, K. R. *Appl. Catal., A* **2001**, *208*, 291.
(10) Li, Y.; Xu, B.; Fan, Y.; Feng, N.; Qiu, A.; Miao, J.; He, J.; Yang, H.; Chen, Y. *J. Mol. Catal. A: Chem.* **2004**, *216*, 107.
(11) Jongsomjit, B.; Wongsalee, T.; Praserthdam, P. *Mater. Chem. Phys.* **2005**, *92*, 572.
(12) Jung, K. Y.; Park, S. B. *J. Photochem. Photobiol., A* **1999**, *127*, 117.
(13) Conesa, J. C.; Malet, P.; Unuera, G. M.; Sanz, J.; Soria, J. *J. Phys. Chem.* **1984**, *88*, 2986.
(14) Salama, T. M.; Hattori, H.; Kita, H.; Ebitani, K.; Tanaka, T. *J. Chem. Soc., Faraday Trans.* **1993**, *89* (12), 2067.
(15) Liqiang, J.; Xiaojun, S.; Weimin, C.; Zili, X.; Yaoguo, D.; Honggang, F. *J. Phys. Chem. Solids* **2003**, *64*, 615.
(16) Price, N. J.; Reitz, J. B.; Madix R. J.; Solomon, E. I. *J. Electron Spectrosc. Relat. Phenom.* **1999**, *98*−*99*, 257.
(17) Zhang, F.; Zheng, Z.; Liu, D.; Mao, Y.; Chen, Y.; Zhou, Z.; Yang, S.; Liu, X. *Nucl. Instrum. Methods Phys. Res., Sect. B* **1997**, *132*, 620.
(18) Kumar, P. M.; Badrinarayanan, S.; Sastry, M. *Thin Solid Films* **2000**, *358*, 122.
(19) Charles, E.; Sykes, H.; Tikhov, M. S.; Lambert, R. M. *J. Phys. Chem. B* **2002**, *106*, 7290.
(20) Mahata, N.; Vishwanathan, V. *J. Catal.* **2000**, *196*, 262.

(21) Ali, S. H.; Goodwin, J. G., Jr. *J. Catal.* **1998**, *176*, 3.
(22) Sales, E. A.; Bugli, G.; Ensuque, A.; Mendes, M. J.; Bozon-Verduraz, F.; *Phys. Chem. Chem. Phys.* **1999**, *1*, 491.
(23) Sarkany, A.; Zsoldos, Z.; Furlong, B.; Hightower, J. W.; Guczi, L. *J. Catal.* **1993**, *141*, 566.
(24) Vannice, M. A.; Wang, S. Y.; Moon, S. H. *J. Catal.* **1981**, *71*, 152.
(25) Nag, N. K. *Catal. Lett.* **1994**, *24*, 37.
(26) Aplund, S. *J. Catal.* **1996**, *158*, 267.
(27) Stevenson, S. A.; Dumesic, J. A.; Baker, R. T. K.; Ruckenstein, E. *Metal−Support Interactions in Catalysis, Sintering, and Redispersion*; Van Nostrand Reinhold: New York, 1987.
(28) Benvenutti, E. V.; Franke, L.; Moro, C. C. *Langmuir* **1999**, *15*, 3140.
(29) Panpranot, J.; Nakkararuang, L.; Ngamsom, B.; Praserthdam, P. *Catal. Lett.* **2005**, *103*, 53.